ISSN 2072-5981
doi: 10.26907/mrsej

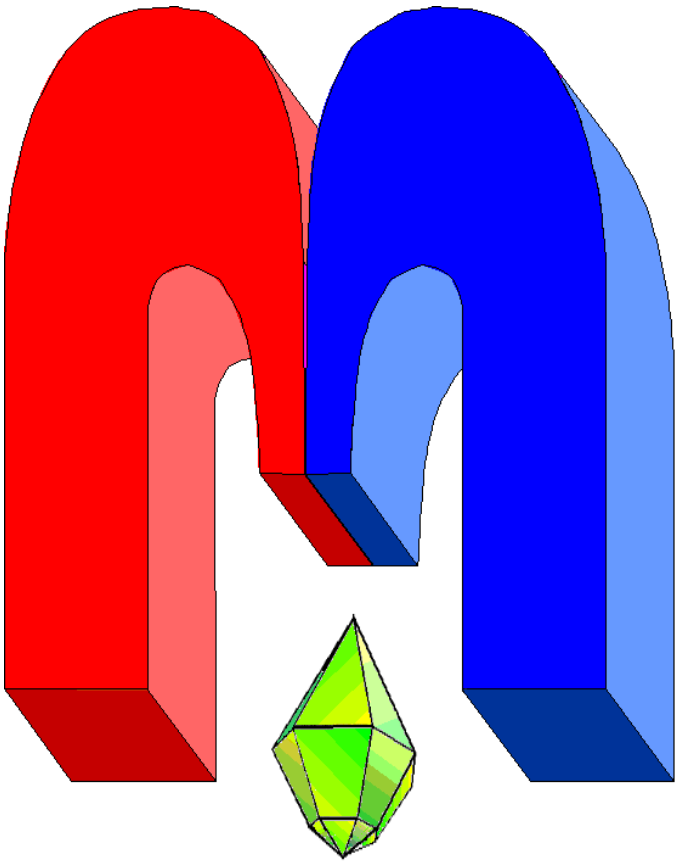

# Magnetic Resonance in Solids

Electronic Journal

*Volume 25*
*Issue 2*
*Article No* ***23203***
*1-6 pages*
***2023***
doi: **10.26907/mrsej-23203**

http://mrsej.kpfu.ru
http://mrsej.ksu.ru

Established and published by Kazan University*
Endorsed by International Society of Magnetic Resonance (ISMAR)
Registered by Russian Federation Committee on Press (#015140), August 2, 1996
First Issue appeared on July 25, 1997



"***Magnetic Resonance in Solids. Electronic Journal***" (**MRS*ej***) is a peer-reviewed, all electronic journal, publishing articles which meet the highest standards of scientific quality in the field of basic research of a magnetic resonance in solids and related phenomena.

Indexed and abstracted by
*Web of Science* (*ESCI*, Clarivate Analytics, from 2015), *Scopus* (Elsevier, from 2012), *RusIndexSC* (*eLibrary*, from 2006), *Google Scholar*, *DOAJ*, *ROAD*, *CyberLeninka* (from 2006), *SCImago Journal & Country Rank*, etc.



* Address: "Magnetic Resonance in Solids. Electronic Journal", Kazan Federal University; Kremlevskaya str., 18; Kazan 420008, Russia

† In Kazan University the Electron Paramagnetic Resonance (EPR) was discovered by Zavoisky E.K. in 1944.

# Low cost ODMR attachment for commercial EPR spectrometers

D.G. Zverev*, F.F. Murzakhanov, M.A. Sadovnikova, B.V. Yavkin

Kazan Federal University, Kremlevskaya 18, Kazan 420008, Russia

**E-mail: dmitry.zverev@gmail.com*

(Received June 30, 2023; revised July 31, 2023;
accepted August 2, 2023; published August 3, 2023)

The low-cost device for optical detection of magnetic resonance (ODMR) has been developed for use with commercial electron paramagnetic resonance spectrometers. The equipment is based on a scheme with coaxial optical fibers, where the excitation is transmitted through a central fiber with a diameter of 400 $\mu$m, and the photoluminescence signal is collected using seven optical fibers with a diameter of 200 $\mu$m. The device has the ability to modulate the excitation radiation, microwave frequency and magnetic field. The ODMR attachment has been tested on standard and well-known $NV^-$ (nitrogen-vacancy) paramagnetic centers in diamonds. ODMR experiments were carried out in the X-band (9.4 GHz) frequency range with a magnetic field $B_0$ sweeping from 220 to 470 mT. The best signal-to-noise ratio was obtained by modulating of the magnetic field.

**PACS:** 07.57.Pt, 42.55.f, 42.60.by

**Keywords:** Electron paramagnetic resonance, EPR, optical polarization, ODMR, $NV^-$ defect

## 1. Introduction

At present, magnetic resonance technique contains well-developed methods for studying the microstructure of intrinsic and impurity centers in various materials. Electron paramagnetic resonance (EPR) is one of them used for characterization of transition or rare-earth metal ions, as well as free radicals and spin labels, for instance, in biomedical applications [1]. Sometimes, by studying the properties of paramagnetic centers, it is possible to refine the crystal structure and its symmetry [2]. EPR spectroscopy also plays an important role in the study of semiconductor crystals containing vacancy-type defects – color centers [3, 4]. Prominent examples are nitrogen-vacancy centers in diamond, as well as silicon vacancy-related defects in silicon carbide. Both considered as promising platforms for the implementation of quantum sensors of magnetic fields, including biosensors with submicron spatial resolution, single-photon sources, and the element base for quantum computers [3]. Comprehensive identification of the microscopic nature, study of the dynamic characteristics (lifetime at the excited state), and the determination of the total spin Hamiltonian values of these centers are commonly performed using a combination of different types of equipment extensions. This approach allow expanding the experimental capabilities of the EPR spectrometer. For example, the electron-nuclear double resonance (ENDOR) method [5] allows indirect observation of nuclear magnetic resonance (NMR) transitions through electron transitions. Moreover, due to the increased gyromagnetic ratio of the electrons with respect to the nuclei, corresponding ENDOR signal is several orders of magnitude stronger than NMR signal and one can detect signals with small electron-nuclear interactions. Thus, it is possible to determine hyperfine and quadrupole splitting constant [6, 7]. Another one method is double electron-electron resonance (DEER) spectroscopy that, for instance, allows direct study of the dipole-dipole interactions between $NV^-$ (nitrogen-vacancy) centers [8]. Thereby, the complex experimental analysis makes it possible to obtain complementary information about the object under study, avoiding the technical limitations of each method separately.

Another spectroscopic method is the optically detected magnetic resonance (ODMR). This method combines the properties obtained by EPR with high sensitivity and selectivity of the photoluminescence signal detection [9, 10]. The ODMR method provides information on the magnetic properties of optically excited donor and acceptor states, that are directly (or sometimes indirectly) involved in spin-dependent radiative recombination processes. ODMR method can be successfully used in study of the shifts and splittings of resonance lines under the influence of magnetic and electric fields (Zeeman and Stark effects). In both cases transitions between energy levels of the system under consideration occur according to the selection rules for magnetic resonance. The essential difference between EPR and ODMR methods consists in the registration and excitation methods used. ODMR experiment is a realization of double resonance, in which electronic transitions between different orbital states are controlled by laser radiation and magnetic transitions by microwave radiation. The main advantages of the ODMR method over the standard EPR technique are: first, significant spin polarization is created without requiring cooling of the medium and transition to the strong magnetic fields [11]. Second, the energy of the microwave quantum (photon) is five orders of magnitude smaller compared to the energy of the optical photon, which makes it difficult to detect it. To date, single-spin microwave detection in some sistems is limited by mK temperatures [12], whereas the ODMR technique routinely allows to register signals down to single emitter even at room temperature, confirming its high sensitivity. However, it should also be noticed that ODMR is characterized by some limitations [13] in its application for the structure under study: system must be compliant to the optical excitation, it is crucial to have effective spin-dependent channels leading to a change in the optical properties of the system when the magnetic resonance condition is fulfilled.

The purpose of this article is to describe developing of ODMR attachment for use in combination with commercial EPR spectrometers operating at various temperatures and microwave bands. The implemented scheme in this work was tested with well-known nitrogen-vacancy ($NV^-$) centers in diamond. $NV^-$ is a paramagnetic center with unique electronic, spin, and optical properties, including stable fluorescent signals [14] and long relaxation times [15, 16]. In addition, it is possible to initialize the spin states of $NV^-$ centers by applying optical excitation and read out the states by measuring intensity of photoluminescence [17]. The $NV^-$ center is an object whose unique properties made it possible to successfully extend the application of ODMR techniques to quantum objects in solids at room temperature. The combination of these properties makes $NV^-$ doped diamond a convenient standard sample for testing ODMR scheme [18]. Other ODMR experiments are described in the review [19].

## 2. Setup description

A coaxial fiber-optic circuit, somewhat similar to the scheme proposed in [20] was chosen as the basis for the attachment for optical detection of magnetic resonance (Figure 1). The excitation radiation is generated by a diode-pumped laser (1), manufactured by CNI Lasers with a wavelength of 532 nm. After modulation by an optical obturator (2), filterring out 1064 nm and collimation (3), the radiation is fed into a tin-coated quartz-quartz optical fiber (4) with outer diameter $d = 400\,\mu$m. Then the radiation supplies the sample located in the microwave resonator of the EPR spectrometer. The photoluminescence generated by the sample is collected by a set of seven optical fibers with diameter $d = 200\,\mu$m located around the excitation fiber. After the excitation band is cut off by a filter with a cutoff wavelength of 650 nm, the collected optical signal is detected using the silicon photodiode (5). The signal from the photodiode is

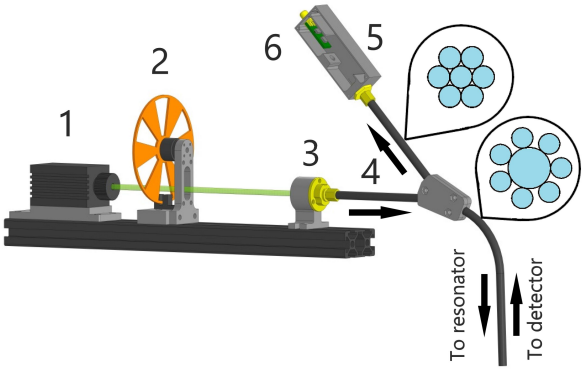


**Figure 1.** Optical part of the ODMR attachment. (1) A 532 nm diode-pumped laser, (2) an optical obturator, (3) 1064 nm filter and collimator, (4) optical fiber 400 $\mu$m, (5) silicon photodiode, (6) preamplifier.

amplified by a preamplifier (6) followed by detection at the modulation frequency using Ametek SR7270 phase detector. In addition to the modulation of optical radiation, our scheme retains the possibility of classical modulation of the magnetic field of the EPR spectrometer, or modulation of the microwave frequency. To detect photoluminescence at certain wavelengths the universal small-sized monochromator is used. At this case the red filter is not required.

The EPR and ODMR spectra were measured on a Bruker ESP300 spectrometer. Measurements in the X-band are carried out using a standard microwave bridge of the spectrometer, whereas the Q-band measurements are carried out using a lab-made one described in previous work [21]. Due to the fact that the sensitivity of the Q-band resonator limits its use, ODMR might significantly expand the spectrometer's capabilities.

## 3. Results and Discussion

To estimate the performance of assembled attachment for ODMR experiments, test measurements on synthetic diamond sample with $NV^-$ centers were performed. Diamond sample was fabricated by Element Six, irradiated by electrons with energy of 2 MeV and flux of $10^{18}$ cm$^{-2}$, followed by annealing at 800°C in two hours to create $NV^-$ centers with a concentration of $1-10$ ppm. The sample is shaped as a thin rectangular prism with size $\approx 3\,\text{mm}\times 2\,\text{mm}\times 0.3\,\text{mm}$, with faces cut perpendicular to [100] direction of diamond cubic lattice. It was glued to the sample holder tube cut by 45° relative to tube axis in order to set [111] crystal direction into the static magnetic field plane. The black curve in the top of figure 2 shows the EPR spectrum of a diamond single crystal in magnetic field orientation close to [111] of the crystal, recorded under continuous optical excitation. The spectrum shows clearly distinguishable signals from the parallel oriented $NV^-$ defects (||) with a splitting between the lines 204.0 mT ($2D \approx 5.7$ GHz), three pairs of lines from other three directions (basal centers) and a signal at $g \approx 2.00$ from the paramagnetic center $N^0$ with the neutral charge state. It can be noticed that the phase of the high-field resonance line $NV^-$ (||), corresponding to the transition $|0\rangle \rightarrow |-1\rangle$, is inverted with respect to the phase of the low-field line of the transition $|0\rangle \rightarrow |+1\rangle$. Continuous optical excitation with following spin-dependent photoluminescence predominantly populate, in our case, ground state spin levels with $M_s = 0$. This process called spin-dependent photoluminescence or optically induced spin polarization [22]. In particular, the difference in the rates of nonradiative relaxations for the electron spin projections $\pm 1$ and 0 of the first optical excited spin triplet leads to the preferential capture of states with the spin projection $\pm 1$ at the long-lived metastable

state. In turn, relaxation from the metastable level to the ground level (also spin triplet) occurs predominantly to the sublevel with the projection $M_s = 0$. As a result, depending on the ratio between the spin-lattice relaxation between $M_s = 0$ and $M_s = \pm 1$ and the power of the exciting laser radiation, full or partial spin polarization of the ground state at the $M_s = 0$ sublevel is achieved. This polarization manifests itself in the EPR spectrum under laser illumination as enhanced absorption (transition $|0\rangle \rightarrow |+1\rangle$) and emission ($|0\rangle \rightarrow |-1\rangle$), which is a phase reversal of the signal, in agreement with experimental observations.

In turn, the ODMR effect in the photoluminescence spectrum of a defect is observed when the transitions between the spin sublevels of the ground level are saturated with resonant microwave radiation, which equalizes the populations of the spin sublevels and, thereby, reduces the PL intensity of the $NV^-$ defect, which is the ODMR signal [23]. The phases of the components in this case are identical, which can be seen in figure 2, the lower graph.

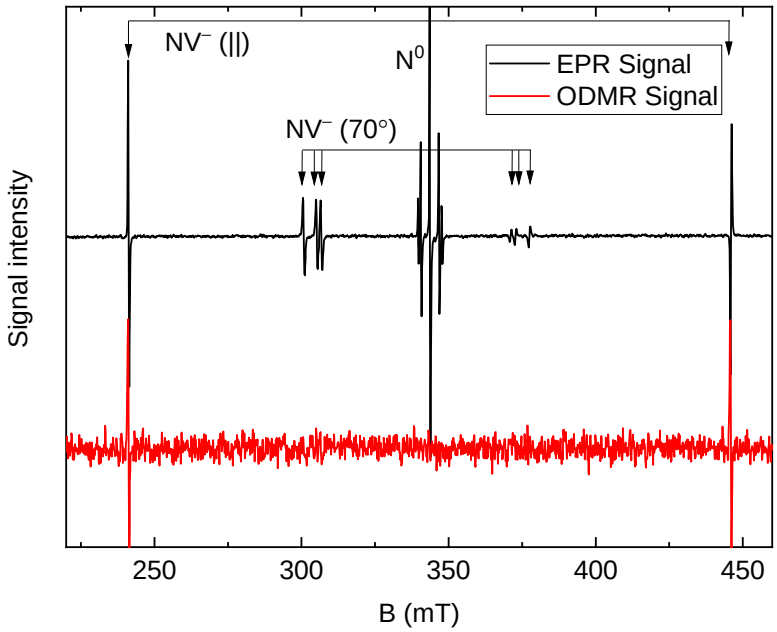


**Figure 2.** EPR (black, top) and ODMR (red, bottom) spectra of single-crystal diamond samples activated by paramagnetic $NV^-$ centers in the orientation [111].

Due to the fact that these changes are relatively small in a bulk sample, various modulation and phase detection techniques are used for measurements to increase the signal-to-noise ratio. In our spectrometer it is possible to modulate the laser source intensity, microwave source (frequency and power) or magnetic field, as in the classical EPR. Modulation of laser light in the case of $NV^-$ defect leads to a significant change in photoluminescence, thus, the detection of an insignificant change in photoluminescence against the background of a strong signal from a synchronous detector is associated with significant difficulties, and slight variations in the parameters lead to strong shift of the baseline of the ODMR spectrum. On the other side, the modulation of the magnetic field, as well as the modulation of microwave radiation during continuous laser illumination of the sample, leads to modulation of the photoluminescence signal against a constant background and can be easily detected using a phase detector.

Red curve in the bottom of figure 2 shows the X-band ODMR signal of $NV^-$ defects in the diamond single crystal with the orientation of magnetic field close to [111] of the crystal under continuous excitation by 532 nm laser radiation and modulation of the magnetic field.

The photoluminescence of the crystal was detected after a red filter with a cutoff wavelength of 650 nm. At the ODMR spectrum one can observe the lines corresponding to the $|0\rangle \rightarrow |+1\rangle$ and $|0\rangle \rightarrow |-1\rangle$ transitions for the parallel orientation of $NV^-$ defects. At the same time, no ODMR signal was detected from the basal centers due to a significant decrease in the ODMR signal intensity when the external magnetic field deviates from the symmetry axis of the defect ([111] axis of the sample), as was shown in [24].

## 4. Conclusion

The article presents the inexpensive ODMR attachment that has been developed for use with commercial electron paramagnetic resonance (EPR) spectrometers. The equipment is based on a scheme with coaxial optical fibers where excitation is transmitted through a central fiber and resulting photoluminescence signal is collected using seven optical fibers around excitation core. The assembled ODMR attachment has the ability to modulate the excitation radiation, microwave frequency and magnetic field that may be necessary for further experiments on different crystals to increase the signal-to-noise ratio. It has been tested on standard and well-known $NV^-$ paramagnetic centers in diamonds. At the spectrum two ODMR lines corresponding to the $|0\rangle \rightarrow |+1\rangle$ and $|0\rangle \rightarrow |-1\rangle$ transitions for the parallel orientation of $NV^-$ defects. The best signal-to-noise ratio was obtained when the modulation of the magnetic field was used.

## Acknowledgments

The work is financially supported by Russian Science Foundation (grant No. 23-22-00271).

## References

1. Bakker M. G., Fowler B., Bowman M. K., Patience G. S., *The Canadian Journal of Chemical Engineering* **98**, 1668 (2020).

2. Loncke F., Zverev D., Vrielinck H., Khaidukov N., Matthys P., Callens F., *Physical Review B* **75**, 144427 (2007).

3. Castelletto S., Boretti A., *Journal of Physics: Photonics* **2**, 022001 (2020).

4. Gracheva I. N., Murzakhanov F. F., Mamin G. V., Sadovnikova M. A., Gabbasov B. F., Mokhov E. N., Gafurov M. R., *The Journal of Physical Chemistry C* **127**, 3634 (2023).

5. Murzakhanov F., Yavkin B., Mamin G., Orlinskii S., von Bardeleben H., Biktagirov T., Gerstmann U., Soltamov V., *Physical Review B* **103**, 245203 (2021).

6. Roessler M. M., Salvadori E., *Chemical Society Reviews* **47**, 2534 (2018).

7. Soltamov V. A., Yavkin B. V., Mamin G. V., Orlinskii S. B., Breev I. D., Bundakova A. P., Babunts R. A., Anisimov A. N., Baranov P. G., *Physical Review B* **104**, 125205 (2021).

8. Eichhorn T. R., McLellan C. A., Jayich A. C. B., *Physical Review Materials* **3**, 113802 (2019).

9. Suter D., *Magnetic Resonance* **1**, 115 (2020).

10. Carbonera D., *Photosynthesis research* **102**, 403 (2009).

11. Happer W., *Reviews of Modern Physics* **44**, 169 (1972).

12. Albertinale E., Balembois L., Billaud E., Ranjan V., Flanigan D., Schenkel T., Estève D., Vion D., Bertet P., Flurin E., *Nature* **600**, 434 (2021).

13. Lund A., Shiotani M., *EPR of Free Radicals in Solids I: Trends in Methods and Applications*, Vol. 24 (Springer Science & Business Media, 2012).

14. Gruber A., Drabenstedt A., Tietz C., Fleury L., Wrachtrup J., Borczyskowski C. v., *Science* **276**, 2012 (1997).

15. Gaebel T., Domhan M., Popa I., Wittmann C., Neumann P., Jelezko F., Rabeau J. R., Stavrias N., Greentree A. D., Prawer S. P., Jan Meijer J. T., Philip R H., Wrachtrup J., *Nature Physics* **2**, 408 (2006).

16. Balasubramanian G., Neumann P., Twitchen D., Markham M., Kolesov R., Mizuochi N., Isoya J., Achard J., Beck J., Tissler J., Vincent J., Hemmer P. R., Jelezko F., Wrachtrup J., *Nature materials* **8**, 383 (2009).

17. Jelezko F., Gaebel T., Popa I., Gruber A., Wrachtrup J., *Physical review letters* **92**, 076401 (2004).

18. Babunts R. A., Kramushchenko D. D., Gurin A. S., Bundakova A. P., Muzafarova M. V., Badalyan A. G., Romanov N. G., Baranov P. G., *Physics of the Solid State* **62**, 2024 (2020).

19. Babashah H., Shirzad H., Losero E., Goblot V., Galland C., Chipaux M., *arXiv preprint arXiv:2205.00005* (2022).

20. Janssen G., Bouwen A., Casteels P., Goovaerts E., *Review of Scientific Instruments* **72**, 4295 (2001).

21. Zverev D., Lukin S., Rodionov A., Shurtakova D., Gafurov M., *Magnetic Resonance in Solids. Electronic Journal* **23**, 21201 (2021).

22. Doherty M. W., Manson N. B., Delaney P., Jelezko F., Wrachtrup J., Hollenberg L. C., *Physics Reports* **528**, 1 (2013).

23. Van Oort E., Manson N., Glasbeek M., *Journal of Physics C: Solid State Physics* **21**, 4385 (1988).

24. Tetienne J., Rondin L., Spinicelli P., Chipaux M., Debuisschert T., Roch J., Jacques V., *New Journal of Physics* **14**, 103033 (2012).